Ultrafast Energy-Transfer Dynamics between Block Copolymer and π-Conjugated Polymer Chains in Blended Polymeric Systems

Yong Hee Kim and Dongho Kim*

Center for Ultrafast Optical Characteristics Control and Department of Chemistry, Yonsei University, Seoul 120-749, Korea

Sae Chae Jeoung*

Laser Metrology Laboratory, Korea Research Institute of Standards and Science, P.O. Box 102, Taejon 305-600, Korea

Ja-Young Han,† Min-Sik Jang, and Hong-Ku Shim*

Department of Chemistry, Korea Advanced Institute of Science & Technology, Taejon 305-701, Korea

Received February 20, 2001. Revised Manuscript Received May 1, 2001

The blending of polymers has been conventionally employed to increase the quantum efficiencies of polymeric electroluminescence (EL) devices via the energy transfer process, which was interpreted in terms of the Förster-type energy transfer based on dipole−dipole interactions. The detailed analysis of various time-resolved spectroscopic data in the blended polymer between MEH-PPV (poly[2-methoxy-5-(2-ethylhexyloxy)-1,4-phenylenevinylene]) and DSiPV (poly[1,3-propanedioxy-1,4-phenylene-1,2-ethylene(2,5-bis(trimethylsilyl)-1,4-phenylene)-1,2-ethylene-1,4-phenylene]) provides some evidence that the ultrafast energy-transfer channel via the shortest interchain distance between the adjacent constituent polymer chains should be considered to account for the dynamics of stimulated emission (SE) and photoinduced absorption (PA) in the blended polymeric systems. These interchain interactions are also responsible for the diminishment of SE of the blended polymer in the transient absorption spectra, because PA is enhanced due to the formation of interchain excitons. These results provide new insight into the role of interchain interactions in the improvement of heteropolymeric EL devices.

Introduction

Conjugated polymers have attracted much research interest in science and technology in the past few decades as semiconductors and electroactive materials for diverse applications in optoelectronics.[1−4] Especially, the electroluminescence (EL) in semiconducting polymers has emerged as a promising application of the polymeric light-emitting diode (LED) because of their advantages such as low cost, facile processing, and easily tunable optical and electrical properties. Although noticeable improvements have been made in many areas for the application of polymeric LEDs, there still remains the challenge of improving the device quantum efficiency. A variety of methods[5,6] used to improve the quantum efficiency of polymeric LEDs include the modification of the chemical structure, energy band level, charge carrier transport, and composition.

Although extensive investigations have been performed to understand the controlling factors governing the overall performances of polymeric EL devices, a decisive explanation has not been fully developed especially due to the complicated nature arising from strong interchain interactions between polymer chains which cannot be avoided in solid thin films.[7] And the degree of interchain interactions is strongly influenced by the solvents and polymer concentrations of the solutions from which the polymers in the solid form are prepared. For instance, the MEH-PPV ((poly[2-methoxy-5-(2-ethylhexyloxy)-1,4-phenylenevinylene]) polymer chain prefers an open and straight conformation in nonpolar solvents such as chlorobenzene, leading to the enhancement of the formation of polymer aggregates. On the contrary, the polymer chain tends to be in a tight coil in polar solvents such as tetrahydrofuran (THF), where the interchain interactions are diminished as compared

* To whom correspondence should be addressed. E-mail: (D.K.) dongho@yonsei.ac.kr, (S.C.J.) scjeoung@kriss.re.kr, (H.-K.S.) hkshim@sorak.kaist.ac.kr.

† Current address: Department of Chemistry, University of California, Los Angeles, CA 90095-1569.

(1) Salaneck, W. R.; Lundstrom, I.; Ranby, B. *Conjugated polymers and Related materials;* Oxford University Press: Oxford, 1993; p 65.
(2) Burroughes, J. H.; et al. *Nature* **1990**, *347*, 539.
(3) Osaheni, J. A.; Jeneke, S. A. *Macromolecules* **1994**, *27*, 739.
(4) Strukelj, M.; Papadimitrakopoulos, F.; Miller, T. M.; Rothberg, L. J. *Science* **1995**, 1969.
(5) Braun, D.; Heeger, A. J. *Appl. Phys. Lett.* **1991**, *58*, 1982.
(6) Parker, I. D.; Pei, Q. *Appl. Phys. Lett.* **1994**, *65*, 1272.
(7) Yan, M.; Rothberg, L. J.; Papadimitrakopoulos, F.; Galvin, M. E.; Miller, T. M. *Phys. Rev. Lett.* **1994**, *72*, 1104.

10.1021/cm010146c CCC: $20.00
Published on Web 07/03/2001

with chlorobenzene.[8] In describing the optical responses of conjugated polymers, the exciton model has frequently been invoked. Within the exciton model, the hole and the electron have a binding energy ranging between 0.5 and 1 eV depending on the degree of charge separation.[9−11] The charge separation occurs significantly so that the electron resides on one chain and the hole on a nearby one, which generates a spatially indirect exciton (polaron pair).[12,13] On the other hand, in the case of small charge separation the excitations exist in the form of an intrachain polaron exciton.[14−16] Thus, the nature of primary excitations (exciton) and the interchain interactions are strongly correlated with each other in determining the fate of excitons in polymeric LED systems. Recently, thorough investigations have been made by the Schwartz group to control the interchain interactions in homopolymeric systems by using a variety of spectroscopic measurements.[17−19]

Meanwhile, blending dye molecules or blocked copolymers of PPV derivatives with conjugated organic polymers enhances both photoluminescence (PL) and EL efficiencies compared to those of homopolymers of PPV derivatives. Thus, by carefully selecting the constituent polymers and adjusting their fractions in the blended polymers which are to be used as the emissive layer in LEDs, one can improve the efficiencies of both carrier injection and transport, resulting in the enhancement of the radiative recombination process in conjugated polymers.[20,21] The previous reports on the photophysical properties of blended polymers suggested that the energy transfer from large-band-gap to small-band-gap polymers occurs via the Förster-type energy transfer based on long-range dipole−dipole interactions.[22] Since the nature of primary excitations in polymers is also dependent on the charge separation and interchain interactions, the interchain interactions between blended polymers should be considered for better understanding of the PL and EL enhancement in the blended polymeric system.

In this work, we investigated the photoexcitation dynamics of a MEH-PPV/DSiPV (DSiPV = poly[1,3-propanedioxy-1,4-phenylene-1,2-ethylene(2,5-bis(trimethylsilyl)-1,4-phenylene)-1,2-ethylene-1,4-phenylene]) blended polymer film[23,24] using femtosecond fluorescence up-conversion and pump−probe spectroscopic techniques to gain further insight into the nature of photoexcitation transfer in a composite conjugated polymeric system. We suggest that the interchain interactions play an important role in the energy-transfer processes because the Förster-type energy transfer stems from dipole−dipole interactions between the adjacent DSiPV and MEH-PPV polymer chains.

Chart 1. Structures of (a) MEH-PPV and (b) DSiPV

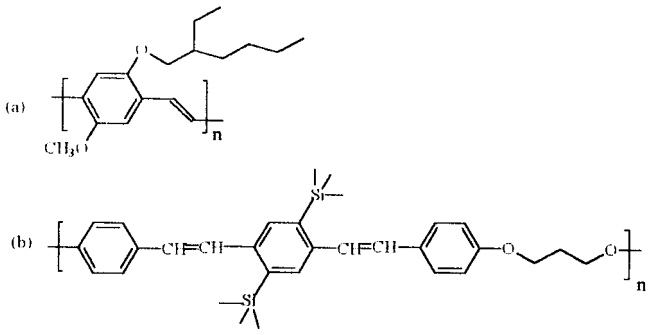

Experimental Section

MEH-PPV and DSiPV were synthesized according to the previously reported method,[23,24] and their structures are shown in Chart 1. Both polymers were dissolved in 1,2-dichloroethane, varying their weight ratios, and then spin-coated on fused silica. In these MEH-PPV/DSiPV films, neither phase separation nor layer formation due to the immiscibility of two polymers has been observed within the allowed spatial resolution (ca. 10 nm) of the atomic force microscope.[26] All the spectroscopic measurements were done under vacuum to avoid photooxidation of the polymeric samples.

The time-integrated PL spectra of various polymer films were recorded with photoexcitations at 325 and 442 nm from a cw He:Cd laser. The PL signal was detected by a combination of a 32 cm focal length monochromator, a Hamamatsu R955 photomultiplier tube, a lock-in amplifier, and a chopper. The picosecond time-resolved PL experiments were carried out by using the time-correlated single-photon counting (TCSPC) method.[27] A cavity-dumped picosecond dye laser (Coherent 702) synchronously pumped by a mode-locked Ar ion laser (Coherent Innova 200) was used to produce a picosecond excitation pulse in the 560−620 nm region and its second harmonics with a β-BBO crystal in the 280−310 nm region. The cavity-dumped beam from the dye laser had a 2 ps pulse width and an average power of ca. 40 mW at a 3.8 MHz dumping rate when rhodamine 6G for gain medium was used. The excitation pulses at 410 nm were obtained from a femtosecond Ti:sappahire laser (Coherent, MIRA) with an average power of 600 mW at 820 nm. The pump pulses at the desired wavelength were generated by frequency doubling with a β-BBO crystal. The emission was collected at a 45° angle with respect to the excitation laser beam by 5 and 25 cm focal length lenses, focused onto a monochromator (Jovin-Yvon HR320), and detected with a microchannel plate photomultiplier tube (Hamamatsu R2809U). The signal was amplified

(8) Nguyen, T. Q.; Doan, V.; Schwartz, B. J. *J. Chem. Phys.* **1999**, *110*, 4068.
(9) Martin, S. J.; Bradley, D. D. C. *Phys. Rev. B* **1999**, *59*, 15133.
(10) Moore, E. E.; Yaron, D. *J. Chem. Phys.* **1998**, *109*, 6147.
(11) Beljonne, D.; Shuai, Z. *J. Chem. Phys.* **1999**, *111*, 2829.
(12) Yan, M.; Rothberg, L. J.; Kwock, E. W.; Miller, T. M. *Phys. Rev. Lett.* **1996**, *76*, 1513.
(13) Berggren, M.; Bergman, P.; Fagerström, J.; Inganäs, Olle; Anderson, M.; Weman, H.; Granström, M.; Stafström, S.; Wennerström, O.; Hjertberg, T. *Chem. Phys. Lett.* **1999**, *304*, 84.
(14) Jenekhe, S. A.; Osaheni, J. A. *Science* **1994**, *265*, 765.
(15) Samuel, I. D. W.; Rumbles, G.; Collison, C. J. *Phys. Rev. B* **1995**, *52*, 11753.
(16) Samuel, I. D. W.; Rumbles, G.; Collison, C. J.; Friend, R. H.; Moratti, S. C.; Holmes, A. B. *Synth. Met.* **1997**, *84*, 497.
(17) Nguyen, T. Q.; Martini, I. B.; Liu, J.; Schwartz, B. J. *J. Phys. Chem. B* **2000**, *104*, 237
(18) Nguyen, T. Q.; Kwong, R. C.; Thompson, M. E.; Schwartz, B. J. *Appl. Phys. Lett.* **2000**, *76*, 2454.
(19) Nguyen, T. Q.; Wu, J.; Doan, V.; Schwartz, B. J.; Tolbert, S. H.; *Science* **2000**, *288*, 652.
(20) Zhang, C.; Seggern, H. Von.; Pakbaz, K.; Kraabel, B.; Schmidt, H. W.; Heeger, A. J. *Synth. Met.* **1995**, *68*, 243.
(21) Nishino, N.; Yu, G.; Heeger, A. J.; Chen, T.-A.; Rieke, R. D. *Synth. Met.* **1995**, *68*, 243.
(22) Förster, T. *Ann. Phys.* **1948**, *2*, 55.
(23) Kang, I.-N.; Hwang, D.-H.; Shim, H.-K.; Zyung, T.; Kim, J.-J. *Macromolecules* **1996**, *29*, 165.
(24) Lee, J.-I.; Kang, I.-N.; Hwang, D.-H.; Shim, H.-K.; Jeoung, S. C.; Kim, D. *Chem. Mater.* **1996**, *8*, 1925.
(25) Wudl, F.; Allemand, D. M.; Srdanov, G.; Ni, Z.; McBranch, D. In *Materials for Nonlinear Optics: Chemical Perspectives*; Marder, S. R., Sohn, J. E., Stucky G. D., Eds.; American Chemical Society: Washington, DC, 1991; p 683.
(26) Heeger, A. J.; Kivelson, S.; Schrieffer, R. J.; Su, W. P. *Rev. Mod. Phys.* **1998**, *60*, 782.
(27) Lee, M.; Kim, D. *J. Opt. Soc. Kor.* **1990**, *1*, 52.

by a wideband amplifier (Philip Scientific), sent to a Quad constant-fraction discriminator (Tennelec), a time-to-amplitude converter (Tennelec), a counter (Ortec), and a multichannel analyzer (Tennelec/Nucleus), and stored in a personal computer for further data processing.

The light source for fluorescence up-conversion measurement[28] was a mode-locked Ti:sapphire laser (Coherent, MIRA-900F) pumped by an intracavity frequency-doubled cw Nd:YVO_4 laser (Coherent, Verdi) with an average power of 600 mW and a ~120 fs pulse width in the 780−900 nm region. The second harmonic pulses were generated by using a β-BBO (1 mm thick) crystal. The residual fundamental pulses after a dichroic mirror were used as the gate pulses for the fluorescence up-conversion. The time interval between the fluorescence and gate pulses was controlled by a delay stage equipped with a corner cube gold retroreflector (Coherent, 2 in. diameter) for traveling the gated pulse. The excitation laser beam was focused onto the sample by using a 5 cm focal length aluminum-coated parabolic mirror. And its power was controlled by using a variable neutral density filter. The fluorescence was collected and focused onto a β-BBO (1 mm thick, type I) crystal for the up-conversion by using two aluminum-coated parabolic mirrors (Coherent, 5 and 20 cm focal lengths). A cutoff filter (Schott Glass Filter Co., GG475, 3 mm thick) was placed between collimating and focusing mirrors to remove the transmitted pump pulse. Up-converted signals were focused onto the entrance slit of a 15 cm focal length monochromator (IBH, 5000M) after passing through a UV bandpass filter (Schott Glass Filter Co., UG11). The signal was detected by a head-on-type photomultiplier tube (Hamamatsu R3235) with a gated photon counter (Stanford Research Systems, SR400). The gated photon counter was interfaced with a personal computer which controls the delay stage. The full width at half-maximum value of the cross-correlation trace between the excitation and gate pulses was estimated to be ~300 fs, which determines the time resolution of the fluorescence up-conversion measurements.

The dual-beam femtosecond time-resolved transient absorption spectrometer[29] consisted of a self-mode-locked femtosecond Ti:sapphire laser (Coherent, MIRA), a Ti:sapphire regenerative amplifier (Quantronix) pumped by a Q-switched Nd:YLF laser, a pulse stretcher/compressor, and an optical detection system. A femtosecond Ti:sapphire oscillator pumped by a cw Nd:YVO_4 laser (Coherent, Verdi) produces a train of ~120 fs mode-locked pulses with an average power of 600 mW at 800 nm. The seed pulses from the oscillator were stretched (~250 ps) and amplified by a Ti:sapphire regenerative amplifier pumped by a Q-switched Nd:YLF laser operating at 1 kHz. After the amplified optical pulses were compressed, the resulting laser beam had a pulse width of ~150 fs and an average power of 800 mW at a 1 kHz repetition rate in the range of 790−840 nm. These pulses were split into two beams by using the beam splitter. One was used as the pump beam by frequency doubling in a β-BBO crystal. The other was focused onto a flowing water cell to generate a white light continuum, which was again split into two parts. One part of the white light continuum was overlapped with the pump beam at the sample to probe the transient, while the other part of the beam was passed through the sample without overlapping the pump beam. The monitoring wavelength was selected by using an appropriate interference filter (fwhm = 10 nm). By chopping the pump pulses at 43 Hz, the modulated probe pulse as well as the reference pulse was detected by two separate photodiodes. The output current was amplified with a homemade fast preamplifier, and then the resultant voltage of the probe pulses was normalized by a boxcar averager with a pulse-to-pulse configuration. The resultant signal modulated by a chopper was measured by a lock-in amplifier and then fed into a personal computer for further signal processing.

(28) Takeuchi, S.; Tahara, T. *J. Phys. Chem. A* **1997**, *101*, 3052.
(29) Jeoung, S. C.; Kim, Y. H.; Kim, D.; Han, J.-Y.; Lee, J.-Y.; Shim, H.-K.; Kim, C. M.; Yoon, C. S. *Appl. Phys. Lett.* **1999**, *74*, 212.

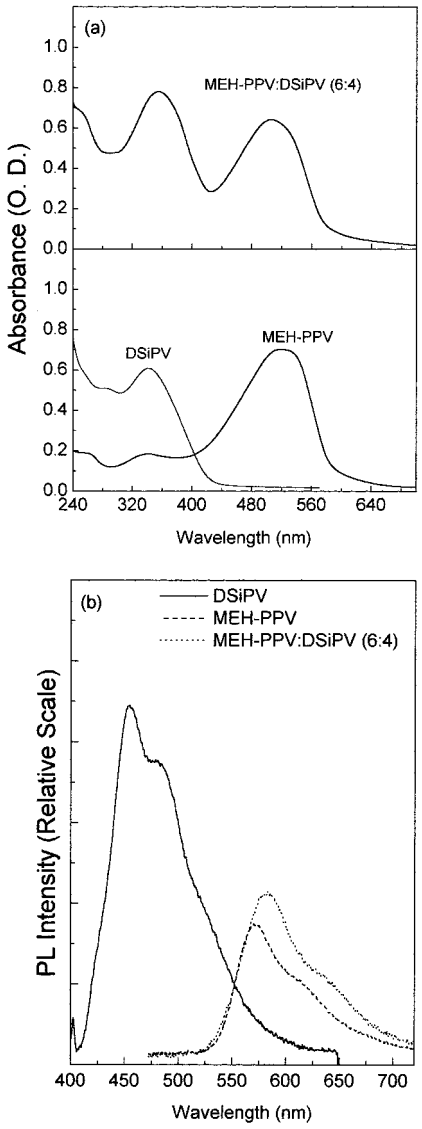

Figure 1. UV−vis absorption (a) and PL (b) spectra of MEH-PPV, DSiPV homopolymers, and MEH-PPV/DSiPV (6:4) blended polymers. The PL spectra were obtained with photoexcitations at 325 nm for DSiPV and MEH-PPV/DSiPV polymer films and at 442 nm for MEH-PPV homopolymer films of thickness ~100 nm by using a cw He:Cd laser.

Results

MEH-PPV and DSiPV homopolymeric films exhibit broad absorption bands due to π-π* transitions around 400−600 and 300−420 nm, respectively. The optical absorption spectrum of a MEH-PPV/DSiPV (6:4 weight ratio) blended polymer, which is satisfactorily derived from a superposition of the absorption spectrum of each constituent polymer, is shown at the top of Figure 1a. This observation reveals that the inhomogeneous broadening due to blending, if any, should be negligible compared with that for each polymer in a solid film. Meanwhile, the observation that neither phase separation nor distinct layer formation from an atomic force microscopy (AFM) image with 10 nm spatial resolution is present in the blended film indicates a good miscibility between the two polymers. Furthermore, the optical density of the blended polymer film is almost identical to the value estimated by using variables such as film thickness, blending ratio, and extinction coefficient for

each constituent polymer. All the observations led us to conclude that neither significant mixing of electronic wave functions nor conformational changes in the ground state occur upon blending.

Figure 1b represents the time-integrated PL spectra upon photoexcitation at 325 or 442 nm for homopolymeric thin films of DSiPV and MEH-PPV and a MEH-PPV/DSiPV (6:4) blended polymer film with maintenance of the film thickness of 100 nm. Assuming the linear absorption within the absorption spectral feature of the blended polymer shown in Figure 1a, the number of photons absorbed by DSiPV overwhelms that by MEH-PPV at the excitation wavelength of 325 nm. The spectral overlap between donor emission (DSiPV, emission in the 400−600 nm region) and acceptor absorption (MEH-PPV, absorption in the 400−600 nm region) is quite large for the effective energy transfer to occur. In fact, the intense PL signal of DSiPV completely disappeared in the 6:4 composite polymer film. Meanwhile, with decreasing the portion of MEH-PPV to 1:9, an apparent PL from DSiPV in addition to that from MEH-PPV was simultaneously observed upon photoexcitation of DSiPV.[24] The strong quenching of DSiPV PL was observed in a wide range of composite ratios between the two polymers upon photoexcitations within π-π^* transitions of DSiPV, implying efficient energy transfer between the two polymers.

It is noteworthy that the time-integrated PL from MEH-PPV in the blended polymer (MEH-PPV/DSiPV) exhibits a prominent red shift of about 10 nm compared with homopolymeric thin films regardless of photoexcitation of DSiPV or MEH-PPV (Figure 1b). The red shift could not be explained in terms of the possible self-absorption around 550 nm because of the lower optical density of the blended polymer at this wavelength. Furthermore, the red shift is not solely due to the dilution effect because no such spectral shift was observed upon diluting MEH-PPV in poly(methyl methacrylate) (PMMA) (6:4 weight ratio), which is optically transparent in the visible region (not shown).

Figure 2 displays the PL decay profiles of MEH-PPV and 1:9 and 1:15 (MEH-PPV/DSiPV) blended polymers (a) and DSiPV and a 1:15 blended polymer (b) with an excitation at 290 nm and a laser fluence of ~0.02 μJ/cm^2. The low excitation density implies negligible contribution of exciton−exciton annihilation processes in the photoexcitation dynamics of polymers. The PL decay profiles of MEH-PPV as well as those of blended polymers detected at 580 nm, which corresponds to the MEH-PPV emission, were fitted with two decay components; the two decay time constants are 20 and 100 ps for MEH-PPV, 50 and 200 ps for a MEH-PPV/DSiPV (1:9) blended polymer, and 200 and 500 ps for a 1:15 blended polymer (Figure 2a). In addition, in the PL decay profiles monitored at 450 nm, which corresponds to the DSiPV emission, the temporal profile of the 1:15 blended polymer shows a faster PL decay than that of DSiPV due to the energy transfer to MEH-PPV (Figure 2b).

Figure 3 represents the PL decay profiles of MEH-PPV and 6:4 (MEH-PPV/DSiPV) blended polymers with two different excitation wavelengths, 307 and 568 nm, and photoexcitation densities of ~0.02 and ~0.1 μJ/cm^2, respectively, which preferentially photoexcite DSiPV and MEH-PPV polymer chains, respectively. Upon photoexcitation of the 6:4 blended polymer at 307 nm, we clearly observed the enhanced PL lifetime of MEH-PPV at 580 nm in the blended polymer as compared with the MEH-PPV homopolymer (Figure 3a). We also measured the PL lifetimes with selective photoexcitation of MEH-PPV polymer chains at 568 nm, which gives a slight increase in the PL lifetimes of MEH-PPV in the blended polymer mainly due to the dilution effect (Figure 3b). The blending of polymers usually induces the dilution effect, which reduces the interchain interactions to generate nonemissive bound polaron pairs between the adjacent polymer chains and consequently enhances the PL efficiency. In other words, the dilution has suppressed energy migration to quenching defects so the solution lifetime of MEH-PPV is recovered. As shown in Figure 3, however, the dilution effect cannot fully explain the enhanced PL lifetimes in the MEH-PPV/DSiPV blended polymeric system. The shorter PL lifetime upon photoexcitation of the MEH-PPV homopolymer with blue excitation at 307 nm as compared with visible excitation at 568 nm is likely to arise from the prominent energy migration process among polymer chains and along the intrachain of MEH-PPV at a high photoexcitation energy (Figure 3a).

It is well established that intrachain excitons produced in polymers are mainly responsible for the PL.

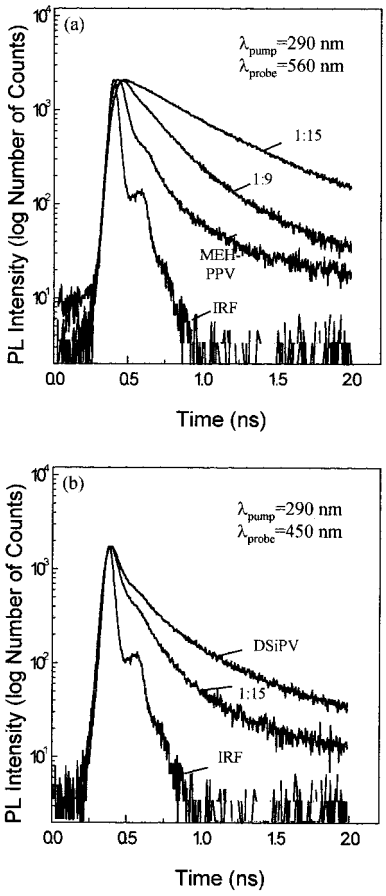

Figure 2. PL decay profiles of MEH-PPV, DSiPV homopolymers, and MEH-PPV/DSiPV (1:9 and 1:15) blended polymers with an excitation at 290 nm and a photoexcitation density of ~0.02 μJ/cm^2 probed at 560 (a) and 450 nm (b) measured by the TCSPC method. The IRF (instrument response function) was obtained by the picosecond pulse scattering, whose fwhm was about 60 ps.

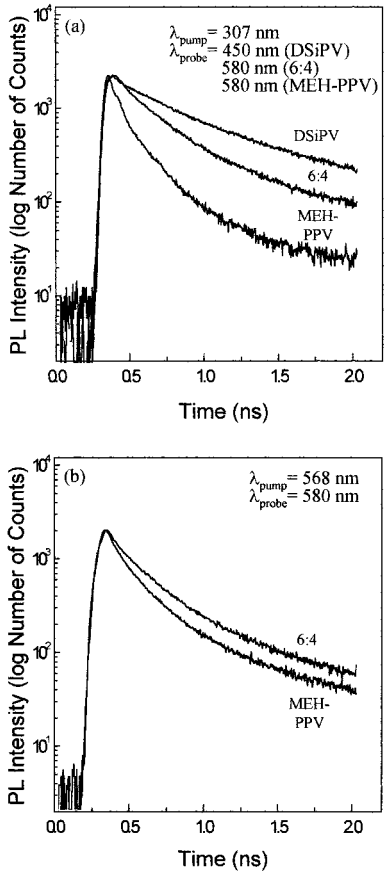

Figure 3. PL decay profiles of MEH-PPV, DSiPV homopolymers, and MEH-PPV/DSiPV (6:4) blended polymer with an excitation at 307 nm and a photoexcitation density of ~0.02 μJ/cm^2 probed at 450 nm for the DSiPV homopolymer and at 580 nm with a photoexcitation density of ~0.1 μJ/cm^2 for the MEH-PPV homopolymer and 6:4 blended polymer (a) obtained by the TCSPC method. PL decay profiles of the MEH-PPV homopolymer and 6:4 blended polymer with an excitation at 568 nm probed at 580 nm (b). The IRF was also displayed for comparison.

Thus, it is important to pursue the formation dynamics of the emissive intrachain excitons in the blended polymers to gain further insight into the energy-transfer processes. For this purpose, we carried out fluorescence up-conversion measurement of the MEH-PPV homopolymer and 6:4 (MEH-PPV/DSiPV) blended polymer (Figure 4). We observed an approximately 200 fs rise time in reaching the maximum PL intensity of the MEH-PPV polymer upon photoexcitation at ~390 nm with an excitation density of ~13 μJ/cm^2 (~3 × 10^{13} photons/cm^2). The relatively low photoexcitation density indicates that the exciton−exciton annihilation process, if any, is not so significant in this experiment. Since the photoexcitation dynamics of π-conjugated polymers are often intensity dependent, the photoexcitation density has been kept as low as possible in our measurements with a relatively large beam diameter of input laser pulses. The ~200 fs time constant is believed to be due to the lattice relaxation process to form the emissive singlet intrachain excitons upon photoexcitation. On the other hand, an about 600 fs rise time was revealed in reaching the maximum PL intensity of MEH-PPV in the 6:4 blended polymer upon photoexcitation at ~390 nm. This gives a time difference of about 400 fs in the formation of the emissive MEH-PPV intrachain singlet

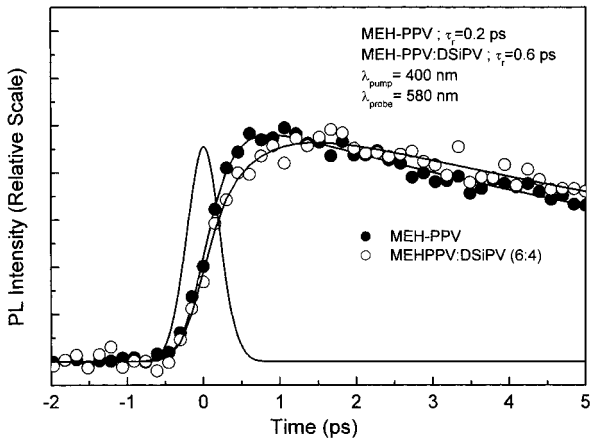

Figure 4. PL temporal profiles of the MEH-PPV homopolymer (filled circles) and MEH-PPV/DSiPV (6:4) blended polymer (open circles) with a ~120 fs pulse excitation at 400 nm and a photoexcitation density of ~13 μJ/cm^2 at 1 kHz probed at 580 nm by the fluorescence up-conversion technique. The cross correlation function between the excitation pulse at 400 nm and the gate pulse at 800 nm is also displayed as a solid line, whose fwhm is about 250 fs.

excitons in the 6:4 blended polymer due to the energy-transfer process from photoexcited DSiPV to MEH-PPV units.

Figure 5a displays the series of transient absorption spectra of MEH−PPV at various time delays between pump and probe pulses with an excitation at 390 nm and an excitation density of ~13 μJ/cm^2 (~3 × 10^{13} photons/cm^2). The main spectral features of these spectra consist of the ground-state bleaching in the 440−600 nm region and the stimulated emission (SE) in the 550−700 nm region. Upon photoexcitation, the bleaching position shifts to lower energy as the time delay increases, finally reaching the maximum intensity at a 0.18 ps delay. In the series of transient absorption spectra of MEH-PPV shown in Figure 5a, it is noteworthy that there is a time lag in the appearance of the SE band in the 550−700 nm region as compared to the instantaneous show-up of a bleaching signal upon photoexcitation. This time lag is attributable to the lattice relaxation process of initially prepared hot photoexcitations to form the intrachain singlet excitons responsible for SE. This is consistent with a ~200 fs rise time in reaching the maximum PL signal as observed in the fluorescence up-conversion measurement (see Figure 4).

Figure 5b shows the series of transient absorption spectra of the 6:4 (MEH-PPV/DSiPV) blended polymer film at various time delays upon photoexcitation at 390 nm with an excitation density of ~13 μJ/cm^2 (~3 × 10^{13} photons/cm^2). Considering the absorption spectra of DSiPV and MEH-PPV, the pump beam at 390 nm corresponds to the tail of the DSiPV absorption spectrum. A broad negative signal ranging from 440 to 600 nm is observed with a spectral change depending on the delay time, which is believed to be due to the combination of the SE of DSiPV mainly appearing in the short-wavelength region and the ground-state bleaching of MEH-PPV in the long-wavelength region in the blended polymer. A much larger ground-state bleaching signal of MEH-PPV (about 4 times) in the transient absorption spectra of the 6:4 blended polymer (Figure 5b) than that

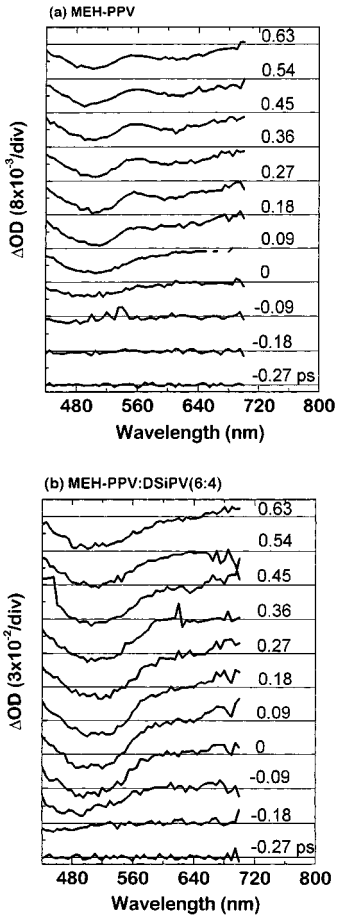

Figure 5. A series of transient absorption spectra of the (a) MEH-PPV homopolymer and (b) MEH-PPV/DSiPV (6:4) blended polymer as a function of the time delay between pump and probe pulses. The other experimental conditions are the same as those in Figure 4.

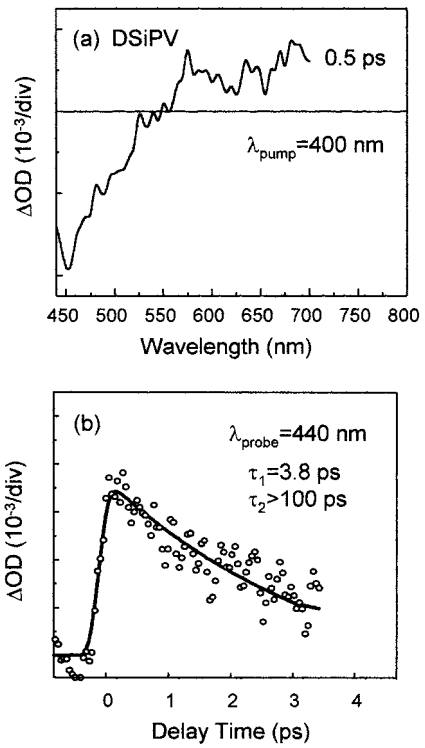

Figure 6. A transient absorption spectrum of the DSiPV homopolymer at a 0.5 ps time delay between pump and probe pulses (a) and the temporal profiles of OD changes at 440 nm, which corresponds to the SE of DSiPV (b). The other experimental conditions are the same as those in Figure 4.

of the MEH-PPV homopolymer (Figure 5a) indicates efficient energy transfer from photoexcited DSiPV to MEH-PPV after predominant excitation of DSiPV chains with 390 nm photoexcitation in the blended polymer. The SE of DSiPV could also contribute, in part, to the negative transient absorption signal lower than 520 nm (see Figure 6a). But as shown in the transient absorption spectra in Figure 5b, its contribution to the negative signal in the region of ground-state bleaching and SE signal of MEH-PPV is negligible. It is noteworthy that the transient absorption signal in the 560−680 nm region is negligible in the MEH-PPV/DSiPV blended polymer as shown in Figure 5b, while the SE signal is prominent in the MEH-PPV homopolymer in the same region (Figure 5a). This behavior could be understood in terms of the competition between the photoinduced absorption (PA) of DSiPV longer than 550 nm (Figure 6a) and the SE of MEH-PPV in the similar spectral region. Since the formation of interchain excitons is promoted in the blended polymer, the diminishment of the SE signal of MEH-PPV in the MEH-PPV/DSiPV blended polymer (Figure 5b) is likely to be due to the enhanced PA signal in the blended polymer. It has been shown that interchain electron−hole pairs have less chance of recombination and are expected to quickly relax and form long-lived defect sites which give rise to the PA signal. Figure 6b shows the temporal behaviors of the SE signals of DSiPV monitored at 440 nm, revealing fast and slow decay components.

Figure 7a shows the temporal profiles of the transient absorption signals of MEH-PPV at various wavelengths. The temporal profiles of bleaching and SE signals exhibit double exponential decay with a detectable rise time at all probe wavelengths except at 440 nm, which corresponds to the bleaching recovery of MEH-PPV. The decay time of the short-lived component is about 1 ps, and that of the long-lived component is about 100 ps. The long-lived component appears to be responsible for the SE lifetime (60−70 ps) being consistent with the PL decay time of MEH-PPV. The short decay time (∼1 ps) is likely to be the decay channel to form polaron pairs. The rise time constant is determined to be $\tau_r = 0.2$ ps by curve fitting analysis, and it is attributable to the lattice relaxation time to form relaxed singlet excitons[30] as observed in the fluorescence up-conversion measurement (Figure 4). The overall decay profiles of the MEH-PPV/DSiPV (6:4) blended polymer also represent double exponential decay (Figure 7b). However, an additional ultrafast decay component ($\tau = 350$ fs) was clearly observed at 440 nm only, which corresponds to the SE of DSiPV, and consequently represents the decay of the singlet polaronic excitons produced in DSiPV. This result suggests that the energy transfer from DSiPV to MEH-PPV in the blended polymer is one of the decay processes of singlet excitons initially prepared in DSiPV units and that this energy-transfer process is responsible for the observed ultrafast decay time constant of

(30) Kersting, R.; Mollay, B.; Rusch, M.; Wenisch, J.; Leising, G.; Kauffman, H. F. *J. Chem. Phys.* **1997**, *106*, 2850.

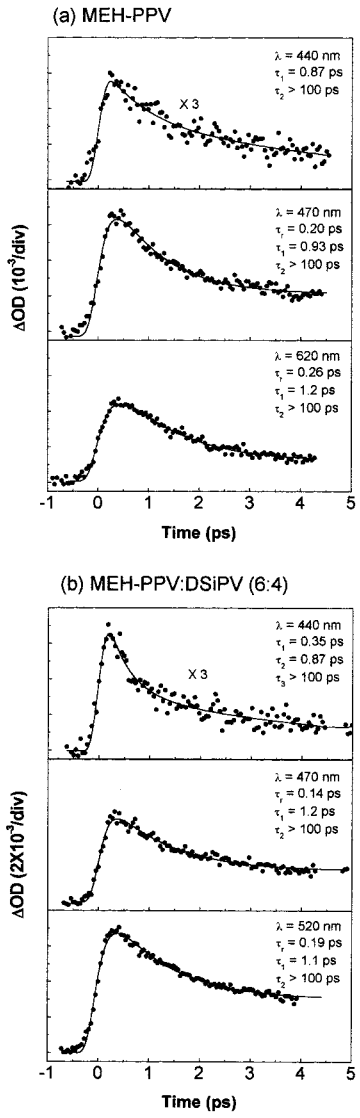

Figure 7. Temporal profiles of OD changes in the transient absorption spectra at various probe wavelengths: (a) MEH-PPV and (b) MEH-PPV/DSiPV (6:4). The other experimental conditions are the same as those in Figure 4.

~350 fs. And the time constant observed in this measurement is consistent with the time lag in reaching the PL maximum in the 6:4 blended polymer revealed by the fluorescence up-conversion experiment (Figure 4).

Discussion

Excitations in π-conjugated polymers undergo incoherent hopping between segments, show spectral diffusion within the density of states (DOS), and can also meet intrinsic or extrinsic traps. The exciton migration in polymer films includes both intra- and interchain excitation hopping. Therefore, the spectral move to lower energy shown in the series of transient absorption spectra is attributable to the energy relaxation among the polymer chains with different effective conjugation lengths.[31−34] Since there is no preferred direction for interchain excitation hopping, 3D migration appears to be more likely. The lower PL quantum efficiency for a solid-state film than that for a diluted organic system leads to the possibility of trapping neutral polaron excitons to defect sites during the cascading relaxation within the DOS.[35] In addition, the charge separation of uncorrelated electron−hole pairs into a charged polaron and bipolaron prior to the formation of the intrachain neutral polaron excitons should be considered.[36]

The previous steady-state and time-resolved PL studies on polymers in various solvents and films indicate strong interchain interactions leading to an excited state that is delocalized over more than one chain and is not strongly radiatively coupled to the ground state. Thus, the exciton binding energy in PPV-type polymers after including interchain interactions has been measured to be 0.7−0.8 eV, whereas the single-chain binding energy can be larger.[9−11] Therefore, the excitations formed on the polymer intrachains can be simply considered as tightly bound static dipoles, leading to bimolecular dipole−dipole interactions. In the case of bimolecular dipole−dipole interactions, the delocalization of two interacting excited states leads to a longer effective range than in the case of the energy-transfer process between two polymers, where only one delocalized excited state is involved. A slightly smaller exciton binding energy including interchain interactions indicates that the interchain exciton delocalization is involved as well as along the chain. In the polymer blends, the interchain interactions can occur between different macromolecules, the degree of which depends on parameters such as interchain distance and geometrical factors between the adjacent polymer chains.

The Förster-type dipole−dipole interaction range can be calculated from the following equation:[22]

$$R_o^{\,6} = \frac{9000 \ln 10 \kappa^2 \eta d}{128 \pi^6 n^4 N_A} \int_0^\infty f_d(\tilde{\nu}) \epsilon_a(\tilde{\nu}) \frac{d\tilde{\nu}}{\tilde{\nu}^4}$$

where $\tilde{\nu}$ is the wavenumber, ϵ_a is the molar decadic extinction coefficient of the acceptor, f_d is the normalized PL spectral distribution of the donor, η_d is the quantum yield of the donor, N_A is Avogadro's number, n is the index of refraction of the blend, and κ^2 is an orientation factor, which in the case of random directional distribution is $^2/_3$. Thus, there are two fundamental requirements for efficient energy transfer via the Förster mechanism: good spectral overlap between the emission of the donor "blue" polymer and the absorption of the acceptor "red" polymer and uniform mixing of the two species. The overlap integral term (J) expresses the degree of spectral overlap between donor emission and acceptor absorption, and the value is calculated to be 1.38×10^{-14} M^{-1} cm^{-3} in the MEH-PPV/DSiPV blended polymer. Good mixing is required since the range of the energy transfer is only a few tens of angstroms. To compare the measured energy-transfer rate with the theoretical predictions, we calculated R_o from the above equation using the spectral overlap J. We obtained R_o

(31) Kersting, R.; Lemmer, U.; Mahrt, R. F.; Leo, K.; Kurz, H.; Bassler, H.; Gobel, E. O. *Phys. Rev. Lett.* **1993**, *70*, 3820.
(32) Warmuth, Ch.; Tortschanoff, A.; Brunner, K.; Mollay, B.; Kauffmann, H. F. *J. Lumin.* **1998**, *76*, *77*, 498.
(33) Bässler, H.; Schweitzer, B. *Acc. Chem. Res.* **1999**, *32*, 173.
(34) van Hutten, P. F.; Brouwer, H. J.; Krasnikov, V. V.; Ouali, L.; S'talmach, U.; Hádziioannou, G. *Synth. Met.* **1999**, *102*, 1443.
(35) Cornil, J.; dos Santos, D. A.; Crispin, X.; Silbey, R.; Brédas, J. L. *J. Am. Chem. Soc.* **1998**, *120*, 1289.
(36) Blatchford, J. W.; Jessen, S. W.; Lin, L. B.; Lih, J. J.; Gustafson, T. L.; Epstein, A. J.; Fu, D. K.; Marsella, M. J.; Swager, T. M.; MacDiarmid, A. G.; Hamaguchi, H. *Phys. Rev. Lett.* **1996**, *76*, 1513.

$= \sim 30$ Å for MEH-PPV/DSiPV blended polymer. But the value of $R_o = \sim 13$ Å was obtained based on the measured energy-transfer rate of ~400 fs in femtosecond fluorescence up-conversion and transient absorption measurements. The ~13 Å center-to-center distance between the MEH-PPV and DSiPV chains in the blended polymer is sufficiently short so that multipole corrections to the dipole−dipole approximations could increase the energy-transfer rate by a factor of 5 or more. These corrections indicate that the through-space Förster-type energy transfer is much more substantial than those in the other blended polymers. To explain the fast energy-transfer behavior of the MEH-PPV/DSiPV (6:4) blended polymer, we estimate the average distance between the acceptor molecules that we refer to the monomer unit that can be excited as $R \approx (N_a(4\pi/3))^{-1/3}$. By accounting for the molecular weight of each monomer unit, we obtained ~5 Å for the 6:4 polymer blend. Thus, the energy transfer is very efficient because the calculated Förster range is much longer (~30 Å).

The energy transfer on the blended polymeric system of *m*-LPPP/PPDB was investigated by Cerullo et al.[37] They have reported that the energy transfer from *m*-LPPP to PPDB takes place on a time scale ranging from 10 to 20 ps at a relatively low concentration of PPDB (about a few percent) depending on the PPDB concentration. In addition, considering the lifetime and the quantum yield of the donor in the absence of an acceptor, which are reported to be 1200 ps and 30%, respectively, the observed energy-transfer rate of 10−20 ps seems to be much faster than the calculated energy-transfer rate of the *m*-LPPP/PPDB blended polymer by the Förster theory, which comes out to be as much as several hundreds of picoseconds. This discrepancy resides on the fact that the interchain distance between energy donor and acceptor chains can be much closer than that calculated by a simple spectral overlap based on a dipole−dipole approximation. In reality, the polymer chain segments can have entangled structures. In addition, the energy donor has a much shorter effective chain length than the energy acceptor chain because the high-energy donor polymer has a shorter π conjugation length. Since the average MW of DSiPV is approximately 4500, this gives rise to ~9 repeating units/chain. This is about 2 orders of magnitude smaller than that of MEH-PPV. Thus, it can be assumed that the short energy donor chain segments can be embedded into the long entangled energy acceptor chains, which results in close contact sites attaining a very short distance between donor and acceptor chains although the average center-to-center distance can be large. As mentioned before, the form of polymers (straight vs entangled) is rather sensitive to the polarities of the solvents employed. For instance, MEH-PPV prefers an entangled structure in THF, leading to a reduction in interchain interactions as compared with chlorobenzene. As the interchain interactions between MEH-PPV chains become stronger, the efficiency of the energy transfer from DSiPV to MEH-PPV in the blended polymer is reduced. On the other hand, as the energy donor polymer chains remain in the form of a tight coil, the energy transfer from the surrounding DSiPV segments becomes slightly enhanced probably because the DSiPV units can exist nearer to the MEH-PPV chains. Indeed the PL decay rate from MEH-PPV at 620 nm in the 6:4 blend film cast from THF solution upon selective photoexcitation of the DSiPV unit at ~300 nm is slightly slower by ~10% than that from chlorobenzene solution (not shown). In addition, the cw PL spectra of the 6:4 blend film prepared from THF solution is slightly shifted and enhanced to the red region as compared with that from chlorobenzene solution. These results indicate that the interchain interactions between MEH-PPV and DSiPV chains as well as among MEH-PPV polymer chains are different depending on the solvents. It is known that the interchain interactions change with film morphology, which gives rise to morphology-dependent aggregates. As the interchain interactions among MEH-PPV polymer chains are stronger, the increasing fraction of aggregates in the film lowers the overall quantum yield for emission than the exciton. The degree of the formation of interchain species is sensitive to the solvents and concentrations of the polymer solutions from which the solid films are prepared. Thus, controlling the interchain interactions is to mediate the energy-transfer processes, which also affects the overall performances of polymeric LED materials. The enhancement of PL quantum efficiency by the dilution effect in the blended polymeric system is believed to be similar to that of energy donor and acceptor polymers regardless of the solvents employed. Overall, we have argued that the blend polymer film prepared from THF solution is advantageous in the efficiency of energy transfer from photoexcited DSiPV as compared with that from chlorobenzene due to the different degrees of interchain interactions among MEH-PPV chains and between DSiPV and MEH-PPV chains.

Summary and Conclusions

In MEH-PPV/DSiPV blended polymers, the PL from DSiPV completely disappears with doping only a few weight percent of MEH-PPV along with the enhancement of PL from MEH-PPV. To investigate the energy-transfer dynamics in the blended polymers, we measured the temporal profiles as well as the spectral changes of PA, SE and spontaneous emission by using various time-resolved spectroscopic methods. We observed an additional ultrafast decaying component of ~350 fs for SE of the large-band-gap conjugated polymer, DSiPV, with mixing with the low-band-gap one, MEH-PPV, upon photoexcitation of DSiPV accompanied by the diminishment of the SE signal for MEH-PPV (Figures 5b and 7b), while SE is evidently detected in the MEH-PPV homopolymeric thin film (Figure 5a).

The detailed analysis of our data based on a variety of time-resolved spectroscopic measurements yields evidence that strong interchain interactions between the adjacent heteropolymeric chains could occur especially through short-range interactions. We also show that the presence of intermolecular interactions between two different chromophores has a strong influence on the formation of the emissive excitons, which causes an apparent enhancement of luminescence quantum efficiency. These interchain polaron pairs are also responsible for the diminishment of SE in the transient

(37) Cerullo, G.; Nisol, M.; Stagira, S.; De Silvestri, S.; Lanzani, G.; Graupner, W.; List, E.; Leising, G. *Chem. Phys. Lett.* **1998**, *288*, 561.

absorption spectra of blended polymers, the red-shifted PL spectra, and the slower PL decay of MEH-PPV upon addition of DSiPV to MEH-PPV. Thus, the overall energy-transfer processes in the blended polymeric system occur through the Förster-type energy-transfer process induced by the strong short-range interchain interactions between energy donor and acceptor polymer chains.

Acknowledgment. This work has been financially supported by Creative Research Initiatives of the Ministry of Science and Technology of Korea (D.K.) and the Center for Advanced Functional Polymers through the KOSEF (H.-K.S.).

Supporting Information Available: Figures showing the PL spectra of MEH-PPV and 6:4 MEH-PPV/DSiPV blend polymer films and PL decay profiles of 6:4 MEH-PPV/DSiPV blend polymer films (PDF). This material is available free of charge via the Internet at http://pubs.acs.org.

CM010146C